Structural Engineering and Mechanics, Vol. 45, No. 5 (2013) 677-691 677
DOI: http://dx.doi.org/10.12989/sem.2013.45.5.677

Pressure loading, end- shortening and through- thickness shearing effects on geometrically nonlinear response of composite laminated plates using higher order finite strip method

Mohammad H. Sherafat[*1], Seyyed Amir M. Ghannadpour[2a] and Hamid R. Ovesy[3b]

[1]*Department of Mechanical Engineering, McGill University, 817Sherbrooke West, Montreal, Canada H3A 2K6*
[2]*Aerospace Engineering Department, Faculty of New Technologies and Engineering, ShahidBeheshti University, G.C, 1983963113 Tehran, Iran*
[3]*Aerospace Engineering Department and Centre of Excellence in Computational Aerospace Engineering, Amirkabir University of Technology, Tehran, Iran*

(Received June 9, 2012, Revised December 8, 2012, Accepted February 19, 2013)

Abstract. A semi-analytical finite strip method is developed for analyzing the post-buckling behavior of rectangular composite laminated plates of arbitrary lay-up subjected to progressive end-shortening in their plane and to normal pressure loading. In this method, all the displacements are postulated by the appropriate harmonic shape functions in the longitudinal direction and polynomial interpolation functions in the transverse direction. Thin or thick plates are assumed and correspondingly the Classical Plate Theory (CPT) or Higher Order Plate Theory (HOPT) is applied. The in-plane transverse deflection is allowed at the loaded ends of the plate, whilst the same deflection at the unloaded edges is either allowed to occur or completely restrained. Geometric non-linearity is introduced in the strain–displacement equations in the manner of the von-Karman assumptions. The formulations of the finite strip methods are based on the concept of the principle of the minimum potential energy. The Newton–Raphson method is used to solve the non-linear equilibrium equations. A number of applications involving isotropic plates, symmetric and unsymmetric cross-ply laminates are described to investigate the through-thickness shearing effects as well as the effect of pressure loading, end-shortening and boundary conditions. The study of the results has revealed that the response of the composite laminated plates is particularly influenced by the application of the Higher Order Plate Theory (HOPT) and normal pressure loading. In the relatively thick plates, the HOPT results have more accuracy than CPT.

Keywords: post-buckling; pressure load; Classical Plate Theory (CPT); Higher Order Plate Theory (HOPT); Finite Strip Method (FSM); composite laminated plates

1. Introduction

In various branches of engineering, such as aerospace and marine engineering, composite

[*]Corresponding author, Ph.D. Student, E-mail: mohammad.sherafat@mail.mcgill.ca
[a]Assistant Professor, E-mail: a_ghannadpour@sbu.ac.ir
[b]Professor, E-mail: ovesy@aut.ac.ir

laminated plates and plate structures are increasingly used as structural components. These structures are often employed in situations where they are subjected to in-plane compressive loading. Thus, it is important to accurately predict the buckling and post-buckling behavior of such structures. The post-local-buckling behavior of elastic plates or plate structures is a geometric non-linear problem. The non-linearity occurs as a result of relatively large out-of-plane deflections, which necessitates the inclusion of non-linear terms in the strain-displacement equations. The finite strip method (FSM) is well suited to the accurate and efficient analysis of both single rectangular plates and complicated prismatic plate structures (Cheung 1976). In the field of linear buckling and vibration analysis the method has been developed extensively for the analysis of complicated plate structures formed of composite laminated material having very general material properties. Such development relates to analyses based on the use of both Classical Plate Theory (CPT) and first-order Shear Deformation Plate Theory (FSDT) (Dawe and Peshkam 1989, Dawe and Craig 1988, Dawe and Peshkam1990, Peshkam and Dawe1989, Dawe and Peshkam1990). In the context of CPT, and for homogeneous materials only, the finite strip method has been employed in geometrically non-linear analyses (Graves-Smith and Sridharan1978, Sridharan and Graves-Smith 1981, Hancock 1981, Bradford and Hancock 1984). These works are concerned with the prismatic plate structures as well as single plates, and have concentrated on post-local-buckling behavior. Through-thickness shear effects have been included in geometrically non-linear finite strip analysis by employing the first-order FSDT in considering the large deflection of isotropic plates (Azizian and Dawe 1985, Dawe and Azizian 1986). Finite strip approach has been implemented on the non-linear response of laminates subjected to progressive uniform end shortening, using both CPT and FSDT (Dawe *et al*. 1992, Lam *et al*. 1993, Wang and Dawe 1999). Allowance has been made for general lamination, including anisotropy and bending-stretching material coupling. Finally, for the readers' information, it is noted that a good state-of-the-art summary of the use of the finite strip method in composite plates has been provided (Dawe 2002). Recently, several contributions have been made by developing two different versions of finite strip method, namely semi-analytical (S-a FSM) and spline finite strip methods and applied to the analysis of the geometrically non-linear response of flat, (Ovesyand Ghannadpour 2005, Ovesy *et al*. 2005) or imperfect rectangular composite laminated plates of arbitrary lay-up to progressive end-shortening in their plane (Ovesy *et al*. 2005). The non-linear response of thin laminates subjected to progressive uniform end shortening and normal pressure loading, using CPT finite strip approach has been studied (Ovesy *et al*. 2006).

Large deflection of functionally graded plates under pressure loads and also post-buckling stiffness of I-sections and isotropic plates have been investigated before by using finite strip method (Ovesyand Ghannadpour 2007, Ghannadpour and Ovesy 2008, Ovesy and Ghannadpour 2009). Recently, in the case of composite plates buckling, the higher order semi-analytical finite strip has been implemented in linear analysis of the composite plates (Ovesy *et al*. 2010). Another higher order method called zigzag plate theory and spline finite strip are used for analysis of composite plates (Akhras and Li 2007). This type of FSM is recently developed for piezoelectric composite plates to analyze free vibration and stability (Akhras and Li 2011). In buckling and post-buckling analysis of anisotropic laminated thin shells with external pressure loading, a boundary layer theory is also extended when subjected to axial compression and also external pressure (Shen 2008a, b). Also nonlinear analysis of moderately thick anisotropic laminated cylindrical shell of finite length subjected to lateral pressure, hydrostatic pressure and external liquid pressure has been investigated (Li and Lin 2010).

More recently, for nonlinear response of laminated plates, the effect of in-plane deformation

has been investigated when the structure is subjected to dynamic loads (Kazancı and Turkmen 2012). A new element called higher-order triangular plate bending element is already used for analyzing sandwich plates and laminated composites (Rezaiee *et al*. 2012).

In the current paper, the application of the semi-analytical finite strip method (S-a FSM) is extended to the analysis of non-linear behavior of thin or thick rectangular isotropic/ laminated plates with different boundary conditions when subjected to uniform end shortening in their plane and normal pressure loading. The theoretical developments of the semi-analytical finite strip method are based on the concept of the Higher Order Plate Theory (HOPT), which incorporate additional degrees of freedom for each nodal line. Therefore, this method is more universal in dealing with different plate thicknesses and has more accuracy in comparison with CPT method, specifically in the relatively thick plates.

2. Theoretical development

In this section, the fundamental elements of the theory of the developed finite strip method (FSM) are briefly outlined. It is noted that a composite material and a perfectly flat finite strip are assumed throughout the theoretical developments of this paper. Moreover, the finite strips are assumed to be simply supported out-of-plane at the loaded ends where the in-plane lateral deflection is allowed to occur. Fig. 1 shows a typical finite strip which forms part of a rectangular plate of length A and width B (with $B \geq b$). The edges running parallel to the y-axis are assumed to be subjected to a uniform end-shortening loading. As a result of the HOPT assumption (Reddy 2004)

$$\begin{aligned} u(x,y,z) &= u_0(x,y) + z\phi_x(x,y) - z^3\frac{4}{3h^2}(\phi_x + \frac{\partial w_0}{\partial x}), \\ v(x,y,z) &= v_0(x,y) + z\phi_y(x,y) - z^3\frac{4}{3h^2}(\phi_y + \frac{\partial w_0}{\partial y}), \quad w(x,y,z) = w_0(x,y). \end{aligned} \tag{1}$$

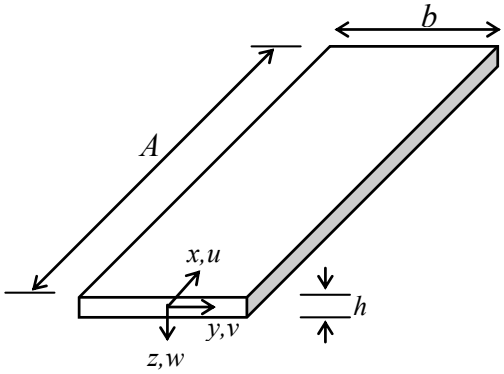

Fig. 1 A typical finite strip

Where u, v and w are components of displacement at a general point, whilst u_0, v_0 and w_0 are similar components at the middle surfaces (z = 0). The quantities ϕ_x and ϕ_y are the rotations of the initial normals to the mid-plane about y and x directions respectively. It is noted that if $\phi_x = -\partial w_0 / \partial x$ and $\phi_y = -\partial w_0 / \partial y$ the Higher Order Plate Theory (HOPT) changes to Classical Plate Theory (CPT). Using Eq. (1) in the Green's expressions for in-plane non-linear strains and neglecting lower-order terms in a manner consistent with the usual von-Karman assumptions, the following expressions for strains at a general point are obtained.

$$\begin{aligned} \{\varepsilon\} &= \{\varepsilon^{(0)}\} + z\{\varepsilon^{(1)}\} + z^3\{\varepsilon^{(3)}\}, \\ \{\gamma\} &= \{\gamma^{(0)}\} + z^2\{\gamma^{(2)}\}. \end{aligned} \tag{2}$$

$$\begin{aligned} \{\varepsilon^{(0)}\} &= \{\varepsilon_l^0\} + \{\varepsilon_{nl}^0\} = \begin{Bmatrix} \dfrac{\partial u_0}{\partial x} \\ \dfrac{\partial v_0}{\partial y} \\ \left(\dfrac{\partial u_0}{\partial y} + \dfrac{\partial v_0}{\partial x}\right) \end{Bmatrix} + \begin{Bmatrix} \dfrac{1}{2}\left(\dfrac{\partial w_0}{\partial x}\right)^2 \\ \dfrac{1}{2}\left(\dfrac{\partial w_0}{\partial y}\right)^2 \\ \left(\dfrac{\partial w_0}{\partial x}.\dfrac{\partial w_0}{\partial y}\right) \end{Bmatrix}, \quad \{\varepsilon^{(1)}\} = \begin{Bmatrix} \varepsilon_{xx}^{(1)} \\ \varepsilon_{yy}^{(1)} \\ \gamma_{xy}^{(1)} \end{Bmatrix} = \begin{Bmatrix} \dfrac{\partial \phi_x}{\partial x} \\ \dfrac{\partial \phi_y}{\partial y} \\ \dfrac{\partial \phi_x}{\partial y} + \dfrac{\partial \phi_y}{\partial x} \end{Bmatrix}, \\ \{\varepsilon^{(3)}\} &= \begin{Bmatrix} \varepsilon_{xx}^{(3)} \\ \varepsilon_{yy}^{(3)} \\ \gamma_{xy}^{(3)} \end{Bmatrix} = -C_1 \begin{Bmatrix} \dfrac{\partial \phi_x}{\partial x} + \dfrac{\partial^2 w_0}{\partial x^2} \\ \dfrac{\partial \phi_y}{\partial y} + \dfrac{\partial^2 w_0}{\partial y^2} \\ \dfrac{\partial \phi_x}{\partial y} + \dfrac{\partial \phi_y}{\partial x} + 2\dfrac{\partial^2 w_0}{\partial y \partial x} \end{Bmatrix}, \begin{Bmatrix} \gamma^{(0)}{}_{yz} \\ \gamma^{(0)}{}_{xz} \end{Bmatrix} = \begin{Bmatrix} \phi_y + \dfrac{\partial w_0}{\partial y} \\ \phi_x + \dfrac{\partial w_0}{\partial x} \end{Bmatrix}, \begin{Bmatrix} \gamma^{(2)}{}_{yz} \\ \gamma^{(2)}{}_{xz} \end{Bmatrix} = -C_2 \begin{Bmatrix} \phi_y + \dfrac{\partial w_0}{\partial y} \\ \phi_x + \dfrac{\partial w_0}{\partial x} \end{Bmatrix}. \end{aligned} \tag{3}$$

Where C_1, C_2 are stated as $C_1 = 4/3h^2$, $C_2 = 3C_1 = 4/\mathrm{h}^2$. The stress-strain relationship at a general point for the plate becomes

$$\begin{Bmatrix} \sigma_{xx} \\ \sigma_{yy} \\ \tau_{yz} \\ \tau_{xz} \\ \tau_{xy} \end{Bmatrix} = \begin{bmatrix} \overline{Q}_{11} & \overline{Q}_{12} & & symm & \\ \overline{Q}_{21} & \overline{Q}_{22} & & & \\ 0 & 0 & \overline{Q}_{44} & & \\ 0 & 0 & \overline{Q}_{45} & \overline{Q}_{55} & 0 \\ \overline{Q}_{61} & \overline{Q}_{62} & 0 & 0 & \overline{Q}_{66} \end{bmatrix} \begin{Bmatrix} \varepsilon_{xx} \\ \varepsilon_{yy} \\ \gamma_{yz} \\ \gamma_{xz} \\ \gamma_{xy} \end{Bmatrix}. \tag{4}$$

Where $\overline{Q}_{ij}(i, j = 1,2,6)$ are plane-stress stiffness coefficients and $\overline{Q}_{ij}(i, j = 4,5)$ are through-thickness shear stiffness coefficients. The constitutive equations for a plate can be obtained through the use of Eqs. (2) to (4) and appropriate integration through the uniform thickness. These equations can be of a very general form which includes general anisotropy and full coupling between in-plane and out-of-plane behaviors and now extended to account for the through-thickness shear effect. The stress resultants are achieved by

$$\begin{Bmatrix} N_{xx} \\ N_{yy} \\ N_{xy} \end{Bmatrix} = \int_{-\frac{h}{2}}^{\frac{h}{2}} \begin{Bmatrix} \sigma_{xx} \\ \sigma_{yy} \\ \tau_{xy} \end{Bmatrix} dz, \quad \begin{Bmatrix} M_{xx} \\ M_{yy} \\ M_{xy} \end{Bmatrix} = \int_{-\frac{h}{2}}^{\frac{h}{2}} \begin{Bmatrix} \sigma_{xx} \\ \sigma_{yy} \\ \tau_{xy} \end{Bmatrix} z dz \ , \quad \begin{Bmatrix} P_{xx} \\ P_{yy} \\ P_{xy} \end{Bmatrix} = \int_{-\frac{h}{2}}^{\frac{h}{2}} \begin{Bmatrix} \sigma_{xx} \\ \sigma_{yy} \\ \tau_{xy} \end{Bmatrix} z^3 dz \ ,$$

$$\begin{Bmatrix} Q_{xz} \\ Q_{yz} \end{Bmatrix} = \int_{-\frac{h}{2}}^{\frac{h}{2}} \begin{Bmatrix} \tau_{xz} \\ \tau_{yz} \end{Bmatrix} dz, \begin{Bmatrix} R_{xz} \\ R_{yz} \end{Bmatrix} = \int_{-\frac{h}{2}}^{\frac{h}{2}} \begin{Bmatrix} \tau_{xz} \\ \tau_{yz} \end{Bmatrix} z^2 dz \ , \tag{5}$$

$$\Rightarrow \begin{Bmatrix} \{N\} \\ \{M\} \\ \{P\} \end{Bmatrix} = \begin{bmatrix} [A] & [B] & [E] \\ [B] & [D] & [F] \\ [E] & [F] & [H] \end{bmatrix} \begin{Bmatrix} \varepsilon^{(0)} \\ \varepsilon^{(1)} \\ \varepsilon^{(3)} \end{Bmatrix} \quad , \quad \begin{Bmatrix} \{Q\} \\ \{R\} \end{Bmatrix} = \begin{bmatrix} [A] & [D] \\ [D] & [F] \end{bmatrix} \begin{Bmatrix} \{\gamma^{(0)}\} \\ \{\gamma^{(2)}\} \end{Bmatrix}.$$

And the plate stiffness coefficients are defined as

$$\begin{aligned} \left(A_{ij}, B_{ij}, D_{ij}, E_{ij}, F_{ij}, H_{ij}\right) &= \int_{-\frac{h}{2}}^{\frac{h}{2}} \overline{Q}_{ij}^{(k)} \left(1, z, z^2, z^3, z^4, z^6\right) dz \qquad (i, j = 1,2,6), \\ \left(A_{ij}, D_{ij}, F_{ij}\right) &= \int_{-\frac{h}{2}}^{\frac{h}{2}} \overline{Q}_{ij}^{(k)} \left(1, z^2, z^4\right) dz \qquad\qquad\qquad (i, j = 4,5). \end{aligned} \tag{6}$$

The strain energy per unit volume is $1/2\sigma^T\varepsilon$. Using Eqs. (2) and (4) to form the strain energy and integrating through the thickness with respect to z gives an expression for the strain energy of the finite strip which can be put into the form

$$\begin{aligned} U_s = &\frac{1}{2}\iint \{[\varepsilon_l^o]^T [A][\varepsilon_l^o] + [\varepsilon^{(1)}]^T [D][\varepsilon^{(1)}] + 2.[\varepsilon_l^o]^T [B][\varepsilon^{(1)}] - 2.C_1.[\varepsilon_l^o]^T [E][\varepsilon^{(3)}] - 2.C_1.[\varepsilon^{(1)}]^T [F][\varepsilon^{(3)}] \\ &+ C_1{}^2.[\varepsilon^{(3)}]^T [H][\varepsilon^{(3)}] + [\gamma^{(o)}]^T [A][\gamma^{(o)}] - 2.C_2.[\gamma^{(o)}]^T [D][\gamma^{(2)}] + C_2{}^2.[\gamma^{(2)}]^T [F][\gamma^{(2)}]\} dx dy \\ &+ \frac{1}{2}\iint \{2.[\varepsilon_l^o]^T [A][\varepsilon_{nl}^0] + 2.[\varepsilon^{(1)}]^T [B][\varepsilon_{nl}^0] - 2.C_1.[\varepsilon^{(3)}]^T [E][\varepsilon_{nl}^0]\} dx dy + \frac{1}{2}\iint \{[\varepsilon_{nl}^0]^T [A][\varepsilon_{nl}^0]\} dx dy \end{aligned} \tag{7}$$

In the expression for U_s in Eq. (7), there are three contributions that depend upon quadratic, cubic and quartic of the displacements. The uniformly distributed pressure load of intensity P_w acts in the z-direction over the whole strip surface and is of fixed intensity in any particular application, whilst the end-shortening is applied progressively. For any finite strip the change in potential energy of the normal pressure loading during the deformation process is given by Eq. (8) and the total potential energy of any strip is described by

$$V_{sp} = -\int_{-b/2}^{b/2} \int_{0}^{A} w P_w dx dy \quad , \quad V_s = U_s + V_{sp} \tag{8}$$

Solution of the non-linear problem is sought through the application of the principle of Minimum Potential Energy. This, of course, requires the assumption of displacement fields to represent the variations of u_0, v_0 and w_0 over the middle surfaces. Here, the displacement fields adopted for typical finite strip shown in Fig.1 are Eq. (9)

$$u_0 = \varepsilon\left(\frac{A}{2} - x\right) + \sum_{i=1}^{ru} U_i(x) g_i^u(y),\ v_0 = \alpha\varepsilon y + \sum_{i=1}^{rv} V_i(x) g_i^v(y),\ w_0 = \sum_{i=1}^{rw} W_i(x) g_i^w(y)$$
$$\phi_{0y} = \sum_{i=1}^{r\phi_y} \phi_{yi}(x) g_i^{\phi_y}(y)\ ,\ \phi_{0x} = \sum_{i=1}^{r\phi_x} \phi_{xi}(x) g_i^{\phi_x}(y) \tag{9}$$

Where ε is the prescribed end-shorteningstrain and ε is a constant. The $U_i(x)$, $V_i(x), \phi_{xi}(x), \phi_{yi}(x)$ and $W_i(x)$ are longitudinal functions satisfying the kinematics conditions prescribed at the strip ends. These functions could be of a variety of forms, but in the present work they are sine or cosine functions. The $g_i^u(y), g_i^v(y)$, $g_i^{\phi_x}(y)$, $g_i^{\phi_y}(y)$ and $g_i^w(y)$ are transverse polynomial interpolation functions of various types and orders, involving undetermined displacement coefficients. In HOPT analysis, the strain energy expression contains second derivatives of w and first derivative of *u, v* and ϕ_x, ϕ_y. This implies a requirement of C^1 type continuity for w and C^0 type continuity for *u, v* and also ϕ_x, ϕ_y. It means that Hermitian shape functions should be used for *w* and Lagrangian shape function should be used for *u, v* and ϕ_x, ϕ_y in the y direction.

$$\begin{aligned}
&g_i^u(y) = N_1^u(y).u_1 + N_2^u(y).u_2 \quad , \qquad g_i^{\phi_x}(y) = N_1^{\phi_x}(y).\phi_{x1} + N_2^{\phi_x}(y).\phi_{x2}\,,\\
&g_i^v(y) = N_1^v(y).v_1 + N_2^v(y).v_2 \quad , \qquad g_i^{\phi_y}(y) = N_1^{\phi_y}(y).\phi_{y_1} + N_2^{\phi_y}(y).\phi_{y_2}\,,\\
&g_i^w(y) = N_1^w(y).w_1 + N_2^w(y)\theta_1 + N_3^w(y).w_2 + N_4^w(y).\theta_2\,.
\end{aligned} \tag{10}$$

Where $u_1, u_2, \phi_{x1}, \phi_{x2}, v_1, u_2, \phi_{y1}, \phi_{y2}, w_1, \theta_1, w_2$ and θ_2 are the degrees of freedom, and the interpolation functions (N) are defined as

$$\begin{aligned}
&N_1^u(y) = N_1^v(y) = N_1^{\phi_x}(y) = N_1^{\phi_y} = \frac{1}{2}(1-\eta),\\
&N_2^u(y) = N_2^v(y) = N_2^{\phi_x}(y) = N_2^{\phi_y} = \frac{1}{2}(1+\eta),\\
&N_1^w(y) = \frac{1}{4}(2-3\eta+\eta^3), \quad N_2^w(y) = \frac{b}{8}(1-\eta-\eta^2+\eta^3),\\
&N_3^w(y) = \frac{1}{4}(2+3\eta-\eta^3), \quad N_4^w(y) = \frac{b}{8}(-1-\eta+\eta^2+\eta^3).
\end{aligned} \tag{11}$$

Where $\eta = 2y/b$.

Considering the facts that the plate is subjected to uniform end-shortening, as indicated by the presence of the term involving ε in the expression for u_0 in Eq. (9), and is simply supported out-of-plane at its loaded ends, the kinematics conditions at its loaded ends are

$$u = \pm A\frac{\varepsilon}{2}, w = 0, \phi_y = 0 \ \ and \ \ \phi_x \neq 0 \tag{12}$$

Consequently, the longitudinal series in the expression for *u*, *w*, ϕ_y and ϕ_x are defined as

$$U_i(x) = W_i(x) = \phi_{yi} = \sin(\frac{i\pi x}{A}) \ and \quad \phi_{xi} = \cos(\frac{i\pi x}{A}) \tag{13}$$

The kinematics condition for the in-plane lateral deflection v at the loaded ends corresponds to a free boundary condition (i.e., $\tau_{xy} = 0$). Thus, v displacement is defined as follows

$$\mathrm{V}_i(x) = \cos\left(\frac{i\pi x}{A}\right) \tag{14}$$

It is noted that the term corresponding to $i = 0$, i.e., the constant value v_0, is included in $V_i(x)$.The $\alpha\varepsilon y$ term is included in Eq. (9) in order to represent precisely the response of a flat unbuckled plate to uniform end compression so that a trivial primary equilibrium path is invoked without involving any un-prescribed degrees of freedom.

With the establishment of the finite strip displacement fields according to the equations that mentioned above, the potential energy of a strip can ultimately be expressed in the form

$$V_s = -\varepsilon\mathbf{d}_s^T\mathbf{C} + \frac{1}{2}\mathbf{d}_s^T\left(K - \varepsilon K^*\right)\mathbf{d}_s + \frac{1}{6}\mathbf{d}_s^T K_1\mathbf{d}_s + \frac{1}{12}\mathbf{d}_s^T K_2\mathbf{d}_s - \mathbf{d}_s^T\mathbf{P} \tag{15}$$

Here K, K_1, K_2 and K^* are symmetric square stiffness matrices. The coefficients of K and K^* are constant whilst those of K_1 and $K_2$are linear and quadratic functions of the displacements, respectively. The column matrix $\mathbf{d}_s$ contain the strip degrees of freedom. C is a column matrix of constants which becomes a null matrix for isotropic or symmetric orthotropic laminates. In evaluating V_s all integrations in the x and y directions are determined analytically.

For the whole plate, comprising an assembly of finite strips, the total potential energy is simply the summation of the potential energies of the individual finite strips. Correspondingly, whole plate matrices which are equivalent of those appearing in Eq. (15) for the individual finite strip are generated by appropriate summations in the standard fashion. Thus, the potential energy for whole plate can be expressed as

$$\overline{V} = -\varepsilon\overline{\mathbf{d}}^T\overline{\mathbf{C}} + \frac{1}{2}\overline{\mathbf{d}}^T\left(\overline{K} - \varepsilon\overline{K}^*\right)\overline{\mathbf{d}} + \frac{1}{6}\overline{\mathbf{d}}^T\overline{K}_1\overline{\mathbf{d}} + \frac{1}{12}\overline{\mathbf{d}}^T\overline{K}_2\overline{\mathbf{d}} - \overline{\mathbf{d}}^T\overline{\mathbf{P}} \tag{16}$$

Where the over bar indicates a whole plate quantity. The plate equilibrium equations are obtained by applying the principle of minimum potential energy. That is to say the partial differentiation of the plate potential energy with respect to each degree of freedom in turn gives a set of non-linear equilibrium equations

$$-\varepsilon\overline{\mathrm{C}} + (\overline{K} - \varepsilon\overline{K}^* + \frac{1}{2}\overline{K}_1 + \frac{1}{3}\overline{K}_2)\overline{\mathbf{d}} - \overline{\mathbf{P}} = 0 \quad \textit{or} \quad -\varepsilon\overline{\mathrm{C}} + \overline{K}_s\overline{\mathbf{d}} - \overline{\mathbf{P}} = 0 \tag{17}$$

Where $\overline{K}_s$ is the global/structural stiffness matrix, and $\overline{\mathbf{d}}$ is a vector, which includes the degrees of freedom for the whole structure. The latter set of equations needs to be modified by applying the appropriate zero-displacement boundary conditions at the longitudinal exterior edges of the plate (i.e., at the unloaded edges of the plate). After the application of any appropriate zero-displacement boundary conditions, the equations must be solved. In the present study the Newton-Raphson (N-R) iterative procedure is selected for solving the equations. Once the global equilibrium equations are solved and the nodal degrees of freedom are found for a particular prescribed end shortening, it is possible to calculate the displacements $u_0, v_0, \phi_{0x}, \phi_{0y}$ and w_0 at any point in any finite strip using Eq. (9) , and to determine force and moment quantities through use of Eq. (5). In particular, the average longitudinal force, N_{av}, is determined by considering the

membrane stress resultant N_{xx} (given by the first of Eq. (5)) and integrating over the strip middle surface area to give the longitudinal force acting on a strip. Then, the total longitudinal force acting on a plate, corresponding to a prescribed end strain, will imply the summation of such strip end forces, i.e.

$$N_{av} = \frac{-\sum\int_{-b/2}^{b/2}\int_{0}^{A} N_x(x,y)dxdy}{A} \tag{18}$$

3. Application and results

It is noted that the plates are assumed to be simply supported on all edges as far as the out-of-plane deflection is concerned, and a pressure load factor is defined as $Q = 36.09\ P_w A^4/E_2 h^4$. It is also noted that for all examples under consideration the FSM analyses are accomplished by utilizing the series representation in the longitudinal direction of the form sin 2, 4, 6/cos 0, 2, 4, 6/sin1, 3/sin 1, 3/cos 1, 3 for $U_i(x), V_i(x), W_i(x), \phi_{yi}$ and ϕ_{xi} respectively. For comparison purposes, the CPT semi-analytical finite strip analysis is also carried out. In the case of CPT analysis, sin 2, 4, 6/cos 0, 2, 4, 6/sin1, 3 are utilized for $U_i(x)$, $V_i(x)$ and $W_i(x)$ respectively. Moreover, the convergence studies with regard to the number of strips have revealed that 40 finite strips are sufficient to obtain converged results in both cases of HOPT and CPT analyses.

3.1 Isotropic simply-supported square plate

The length to thickness ratio of the plate is A/h = 120 (i.e., the thin plate), and the Poisson ratio is υ = 0.3. It is noted that the assumed boundary conditions are the same as those adopted by Ovesy *et al*. (2006) for the analysis of the same plate. It is emphasized that the lateral expansion of the unloaded edges is completely prevented.

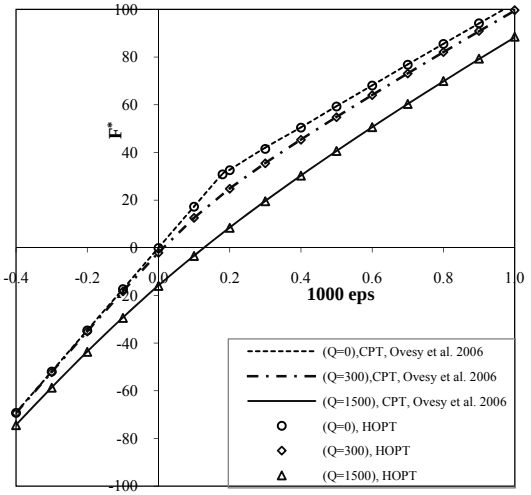

Fig. 2(a) Variation of load factor F* with end-shortening for isotropic thin plate

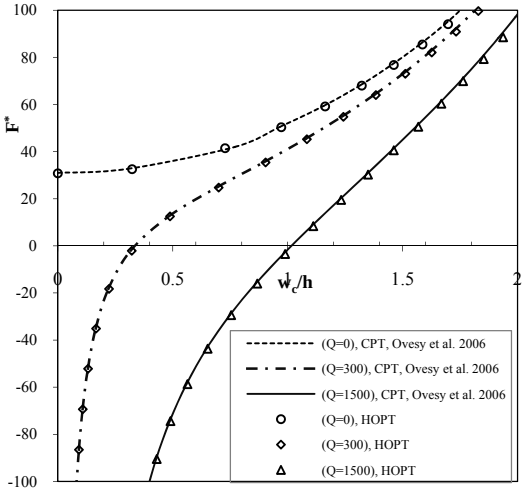

Fig. 2(b) Variation of load factor F* with central deflection for isotropic thin plate

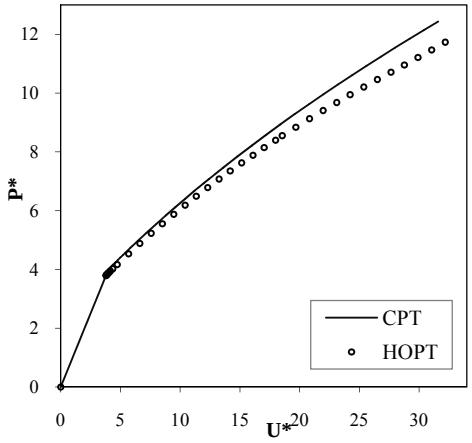

Fig. 3(a) Variation of load factor P* with end-shortening for isotropic thick plate (A/h) = 10

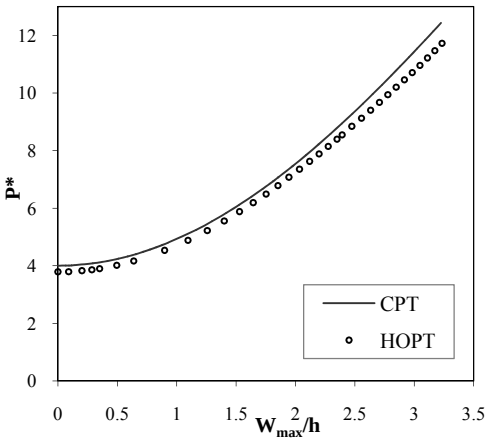

Fig. 3(b) Variation of load factor P* with central deflection for isotropic thick plate (A/h) = 10

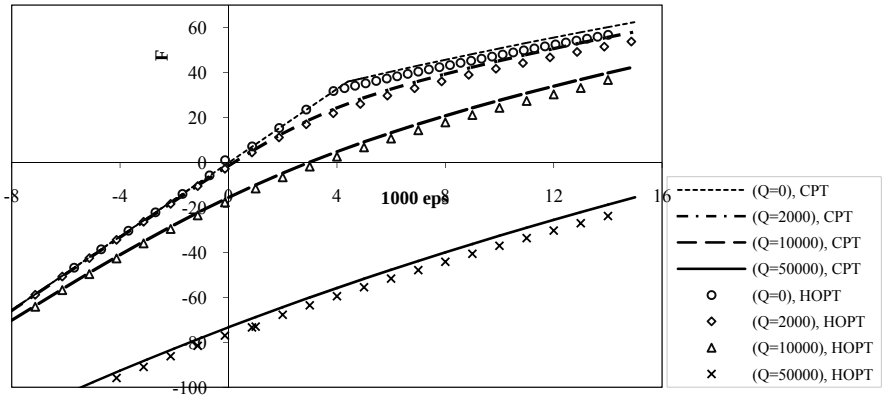

Fig. 4(a) Variation of load factor F with end-shortening for symmetric cross-ply relatively thick laminated (A/h) = 20

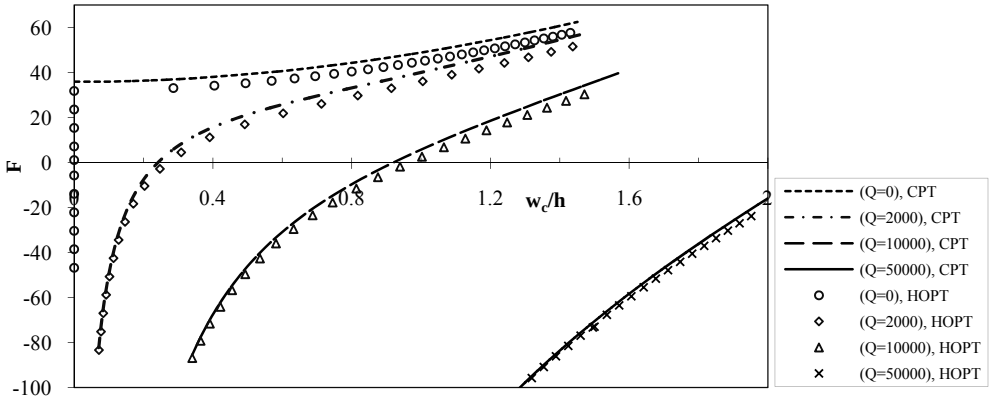

Fig. 4(b) Variation of load factor F with central deflection for symmetric cross-ply relatively thick laminated (A/h)=20

A fixed normal pressure load is applied corresponding to values of a pressure load factor Q of 0, 300 and 1500 in turn, in conjunction with a progressive end-shortening. It is assumed that the pressure load remains constant, whilst the loaded ends progressively approach each other (corresponding to positive ε), or progressively move away from each other (corresponding to negative ε).

In presenting the results a load factor F^*, which is defined as $F^* = 10.92AN_{av}/Eh^3$, is introduced. The variations of load factor with end-shortening and central deflection are depicted in Figs. 2(a) and 2(b) respectively. The results are compared with the corresponding ones, which are obtained based on the CPT assumptions (Ovesy *et al*. 2006). It is clearly seen that the two sets of results compare very closely and thus two methods of HOPT and CPT finite strips have similar results in the cases of thin isotropic plates.

In the case of thick plates with no lateral pressure being applied, Fig. 3(a) shows the variation of the non-dimensional load $P^* = Nav.A/(\pi^2 D)$ with the non-dimensional end-shortening $U^* = \varepsilon A^2 hE/(\pi^2 D)$ for an isotropic thick plate (A/h = 10) with material properties as E = 207000MPa and υ = 0.3. Fig. 3(b) shows the non-dimensional load-peak deflection variations for the same plate. It can be concluded that for the case of thick plates, the present HOPT finite strip method is capable of predicting the post-buckling behavior with a better degree of accuracy compared to that predicted by the CPT finite strip method.

3.2 Symmetric cross-ply square laminate

The symmetrically laminated cross-ply $[0/90]_s$ square plate, which are constructed of plies having the properties $E_1/E_2 = 40$, $G_{12}/E_2 = 0.5$, $G_{23}/E_2 = 0.6$ and $\upsilon_{12} = 0.3$ are studied. The length to thickness ratio of the laminate is A/h = 20 (i.e., relatively thick), and the plies are of equal thickness. The unloaded edges are free to expand laterally in their plane. A fixed normal pressure load is applied corresponding to values of a pressure load factor Q of 0, 2000, 10000 and 50000 in turn, in conjunction with a progressive end-shortening. In presenting the results a load factor F, which is defined as $F = Nav.A/E_2h^3$, is introduced. It is worth noting that in the case of zero normal pressure loading, the laminate is seen to demonstrate a very clear bifurcational characteristic similar to that experienced in Fig. 2(b) with reference to isotropic plate when subjected to zero normal pressure. This occurs due to the bending-stretching coupling terms being zero for the symmetric laminate, allowing the laminate to remain flat before the buckling point is reached. The comparison of the results has indicated that the HOPT assumption has resulted in more accuracy than that obtained by the application of CPT assumptions (Fig. 4(a) and Fig.4 (b)).

3.3 Unsymmetric cross-ply square laminate

In order to verify the results for unsymmetrical laminates, an unsymmetric cross-ply laminate $[0/90]_4$, with material properties: $E_1/E_2 = 40$, $G_{12}/E_2 = 0.5$, $G_{23}/E_2 = 0.6$ and $\upsilon_{12} = 0.3$ is considered. The length to thickness ratio of the laminate is A/h = 20 and the plies are of equal thickness. The boundary conditions for all edges are simply supported give in-plane boundary conditions at the unloaded edges. Figs. 5(a), 5(b) respectively show the non-dimensional load factor $F = Nav.A/E_2h^3$ with the end-shortening and the non-dimensional load factor with central-deflection. The presented results are compared with those obtained by first order shear deformation theory (Wang and Dawe 1999). In both figures, there is good agreement between presented results and the reference.

The square unsymmetric laminate [90/0/90/0], which are constructed of plies having the same

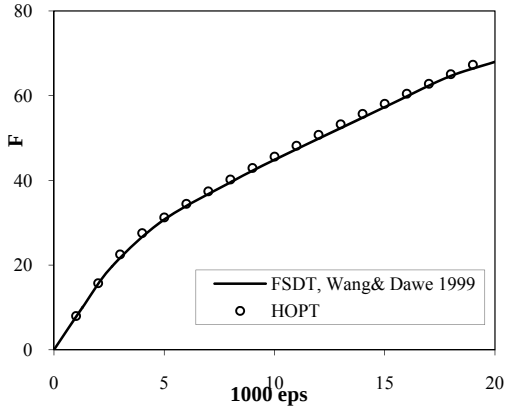

Fig. 5(a) Variation of load factor F with end-shortening for unsymmetric cross-ply relatively thick laminated (A/h) = 20

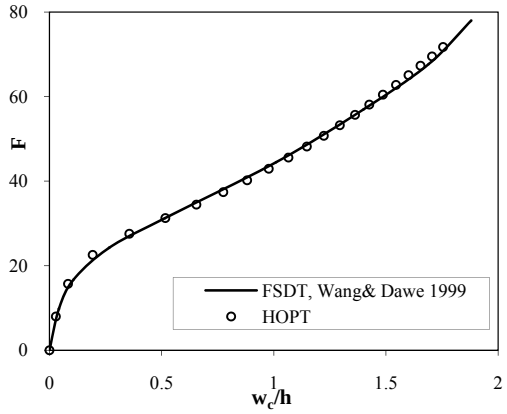

Fig. 5(b) Variation of load factor F with central deflection for unsymmetric cross-ply relatively thick laminated (A/h) = 20

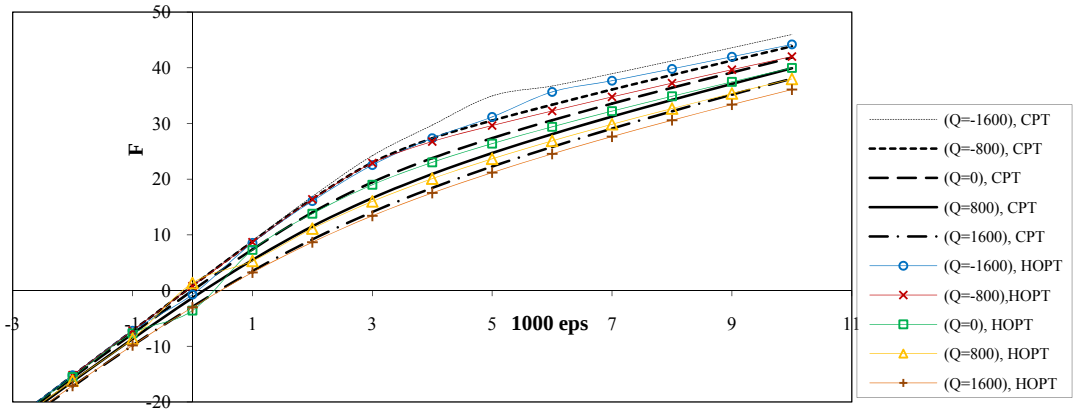

Fig. 6(a) Variation of load factor F with end-shortening for unsymmetric cross-ply relatively thick laminated (A/h) = 20

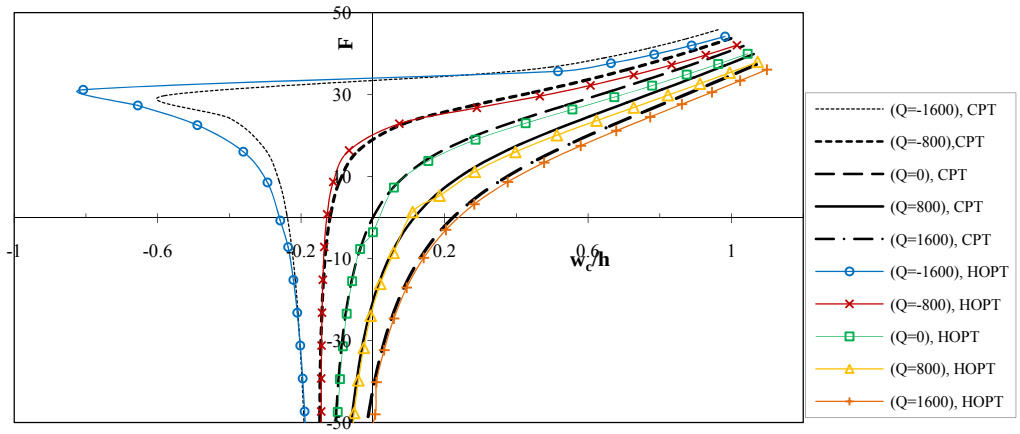

Fig. 6(b) Variation of load factor F with central deflection for unsymmetric cross-ply relatively thick laminated (A/h) = 20

properties as those assumed for the case of symmetric laminate is studied. The length to thickness ratio is A/h = 20 (i.e., relatively thick), and the laminate is composed of equal-thickness layers. It is noted that for this laminate, the non-zero coupling coefficients are B_{11} and B_{22}, with $B_{11} = B_{22}$. The In-plane boundary conditions at the unloaded edges are the same as those considered earlier for the case of symmetric laminate.

A fixed normal pressure load is applied corresponding to values of a pressure load factor Q of -1600, -800, 0, 800 and 1600 in turn, in conjunction with a progressive end-shortening ε. The reason for including both positive and negative pressure load is that the laminate response are expected to be different for positive and negative pressure loadings of equal magnitude, due to the presence of the B_{11} and B_{22} coefficients. In presenting the results, the same load factor F as that adopted earlier for the case of symmetric laminate are considered. The longitudinal force-end shortening and the longitudinal force-central deflection variation are presented in Figs. 6(a) and 6(b), respectively. Once again, the HOPT assumptions have resulted in more accuracy than that obtained by the application of CPT assumptions for the case of relatively thick plate.

It is worth noting that due to the presence of bending-stretching coupling terms, the unsymmetric laminate is seen to demonstrate no bifurcational characteristic for all the cases of normal pressure under consideration, including the case of zero normal pressure loading. It is seen in Fig. 6(b) that for the cases of positive normal pressure loading, i.e., Q = 800 and 1600, where the pressure load produces deflection in the same sense as that produced by the coupling terms for the case of un-pressurized laminate when subjected to positive end-shortening, the interaction between positive pressure loading and the coupling characteristics of the laminate has caused pronounced out-of-plane deflection when the load factor F is positive.

However, a somewhat different behavior is seen to exist for the cases of negative normal pressure loading, i.e., Q = -800 and -1600. That is to say, as the load factor F increases, the negative pressure loading acts against the effects of coupling terms, causing the laminate to remain almost flat in the case of Q = -800, or even to deflect in the negative direction in the case of Q = -1600. However, this kind of behavior is seen to exist up to a certain level of positive load factor F is reached, for a given value of negative normal pressure loading. At this level of load factor F, the fixed normal pressure loading can no longer overcome the coupling effects, and hence the initial load path becomes unstable and the laminate deflects in the positive direction (Fig. 6(b)).

To examine the effects of boundary conditions on the post-buckling behavior, one square unsymmetric laminate [90/0/90/0], which are constructed of plies having the same properties as those assumed for the case of symmetric laminate is studied. The length to thickness ratio is A/h = 20 (i.e., relatively thick), and the laminate is composed of equal-thickness layers. In this case, a fixed normal pressure Q = 800 is applied while the boundary conditions in the y direction are imposed in the form of Eq. (19).

$$
\begin{aligned}
&\text{Simply supported} : y = 0, B: w = 0, \phi_x = 0,\\
&\text{Clamped}: y = 0, B: w = 0, \frac{\partial w}{\partial y} = 0, \phi_x = 0, \phi_y = 0,\\
&\left.\begin{array}{l} x = 0, A: \text{Simply supported} \\ y = 0, B: \text{Simply supported} \end{array}\right\} \Rightarrow \text{i.e.: SSSS}, \quad \left.\begin{array}{l} x = 0, A: \text{Simply supported} \\ y = 0, y = B: \text{Clamped} \end{array}\right\} \Rightarrow \text{i.e.: SCSC},\\
&\left.\begin{array}{l} x = 0, A: \text{Simply supported} \\ y = 0: \text{Simply supported}, y = B: \text{Clamped} \end{array}\right\} \Rightarrow \text{i.e.: SCSS}.
\end{aligned}
\tag{19}
$$

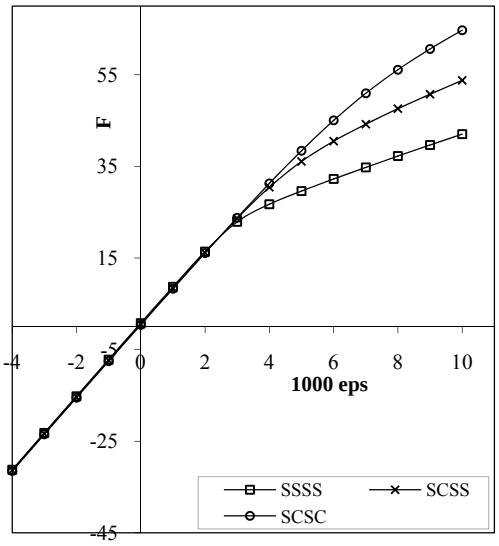

Fig. 7(a) Variation of load factor F with end-shortening for unsymmetric cross-ply relatively thick laminated (A/h) = 20 for different boundary conditions

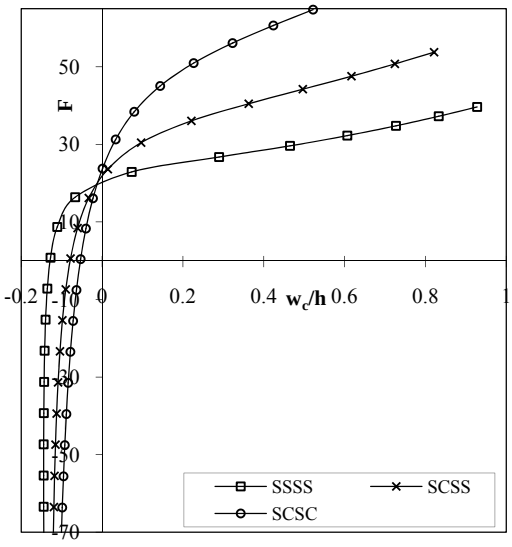

Fig. 7(b) Variation of load factor F with central deflection forunsymmetric cross-ply relatively thick laminated (A/h) = 20 for different boundary conditions

From the presented results in Fig. 7(a) and Fig. 7(b), it is seen that by changing simply supported condition to clamped, plate becomes stiffer and when both unloaded edges are clamped, its response to the pressure loading and end shortening is more different from that with simply supported edges.

4. Conclusions

The application of the semi-analytical finite strip method (S-a FSM) is extended to the analysis of non-linear behavior of thin or thick rectangular composite laminated plates of arbitrary lay-up subjected to progressive end-shortening as well as normal pressure loading. For thin plates, the CPT predicts the post-buckling behavior reasonably accurately. Through the comparison of results, the validity of the formulation of the developed HOPT finite strip methods is approved. The study of the results has revealed that the response of the laminates is significantly influenced by the application of the normal pressure loading. Particularly, the response of unsymmetric laminates is strongly affected by the sign of the normal pressure loading. The results have been compared with FSDT results and the effects of different boundary conditions are also investigated. The post-buckling equilibrium path of laminates under end-shortening is discussed in detail. Moreover, it is revealed that for the case of relatively thick laminate, the HOPT assumptions have resulted in more accuracy than that achieved by the application of CPT assumptions.

References

Azizian, Z.G. and Dawe, D.J. (1985), "Geometrically non-linear analysis of rectangular Mindlin plates using the finite strip method", *Comput. Struct*., **21**, 423-436.
Akhras, G. and Li, W. (2007), "Spline finite strip analysis of composite plates based on higher-order zigzag composite plate theory", *Composite Struct*., **78**, 112-118.
Akhras, G. and Li, W. (2011), "Stability and free vibration analysis of thick piezoelectric composite plates using spline finite strip method", *Int. J. of Mech. Sci*., **53**(8), 575-584.
Bradford, M.A. and Hancock, G.J. (1984), "Elastic interaction of local and lateral buckling in beams", *Thin-walled Struct*., **2**, l-25.
Cheung, Y.K. (1976), *Finite Strip Method in Structural Analysis*, Pergamon Press, Oxford.
Dawe, D.J. (2002), "Use of the finite strip method in predicting the behavior of composite laminated structures", *Composite Struct*. **57**, 11-36.
Dawe, D.J. and Azizian, Z.G. (1986), "The performance of Mindlin plate finite strips in geometrically nonlinear analysis", *Comput.Struct*., **23**, 1-14.
Dawe, D.J. and Craig, T.J. (1988), "Buckling and vibration of shear deformable prismatic plate structures by a complex finite strip method", *Int. J. Mech. Sci.*, **30**, 77-79.
Dawe, D.J., Lam, S.S.E. and Azizian, Z.G. (1992), "Nonlinear finite strip analysis of rectangular laminates under end shortening, using classical plate theory", *Int. J. Numer. Meth. Eng*., **35**, 1087-1110.
Dawe, D.J. and Peshkam, V. (1989), "Buckling and vibration of finite-length composite prismatic plate structures with diaphragm ends, Part I: Finite strip formulation", *Comp. Meth. Appl. Mech. Eng.*,**77**, l-30.
Dawe, D.J. and Peshkam, V. (1990), "Buckling and vibration of long plate structures by complex finite strip methods", *Int. J. Mech Sci*.,**32**, 743-766.
Dawe, D.J. and Peshkam, V. (1990), "A buckling analysis capability for use in the design of composite prismatic plate structures", *Composite Struct*., **16**, 33-63.
Ghannadpour, S.A.M. and Ovesy, H.R. (2008), "An exact finite strip for the calculation of relative post-buckling stiffness of I-section struts", *Int. J. of Mech. Sci*., **50**(9), 1354-1364.
Graves-Smith, T.R. and Sridharan, S. (1978), "A finite strip method for the post-locally-buckled analysis of plate structures", *Int. J. Mech. Sci*., **20**, 833-842.
Hancock, G.J. (1981), "Nonlinear analysis of thin-walled sections in compression", *J. Struct. Eng. Div., ASCE,* **107**, 455-471.
Kazancı, Z. and Turkmen, H.S. (2012), "The effect of in-plane deformations on the nonlinear dynamic response of laminated plates", *Struct Eng. Mech*., **42**(4), 589-608.
Lam, S.S.E., Dawe, D.J. and Azizian, Z.G. (1993), "Nonlinear analysis of rectangular laminates under end shortening, using shear deformation plate theory", *Int. J. Numer. Meth. Eng.*, **36**, 1045-1064.
Li, Z. and Lin, Z. (2010), "Non-linear buckling and post-buckling of shear deformable anisotropic laminated cylindrical shell subjected to varying external pressure loads", *Composite Struct*., **92**, 553-567.
Ovesy, H.R. and Ghannadpour, S.A.M. (2005), "Non-linear analysis of composite laminated plates under end shortening using finite strip method", *Proceedings of the 4th Australasian congress on applied mechanics*, Melbourne, Australia.
Ovesy, H.R. and Ghannadpour, S.A.M. (2007), "Large deflection finite strip analysis of functionally graded plates under pressure loads", *Int. J. Struct. Stability Dynamic*, **7**(2), 193-211.
Ovesy, H.R. and Ghannadpour, S.A.M. (2009), "An exact finite strip for the calculation of relative post-buckling stiffness of isotropic plates", *Struct. Eng. Mech*., **31**(2), 181-210.
Ovesy, H.R., Ghannadpour, S.A.M. and Morada, G. (2005), "Post-buckling analysis of composite laminated plates, using finite strip method", *Proceedings of the 5th international conference on composite science and technology*, Sharjah, UAE.
Ovesy, H.R., Ghannadpour, S.A.M. and Morada, G. (2005), "Geometric non-linear analysis of composite laminated plates with initial imperfection under end shortening, using two versions of finite strip method", *Composite Struct*., **71**, 307-314.
Ovesy, H.R., Ghannadpour, S.A.M. and Morada, G. (2006), "Post-buckling behavior of composite laminated plates under end shortening and pressure loading, using two versions of finite strip method", *Composite Struct*., **75,** 106-113.

Ovesy, H.R., Ghannadpour, S.A.M. and Sherafat, M.H. (2010), "Buckling analysis of laminated composite plates using higher order Semi – analytical finite strip method", *Applied Composite Materials*, **17**, 69-80.

Peshkam, V. and Dawe, D.J. (1989), "Buckling and vibration of finite-length composite prismatic plate structures with diaphragm ends, Part II: computer programs and buckling applications", *Comp. Meth. Appl. Mech. Eng*., **77**, 227-252.

Reddy, J.N. (2004), *Mechanics of laminated composite plates and shells, Theory and Analysis*, Texas.

Rezaiee-Pajand, M., Shahabian, F. and Tavakoli, F.H. (2012), "A new higher-order triangular plate bending element for the analysis of laminated composite and sandwich plates", *Struct. Eng. Mech*., **43**(2), 253-271.

Shen, H. (2008), "Boundary layer theory for the buckling and post-buckling of an anisotropic laminated cylindrical shell. Part I: Prediction under axial compression", *Composite Struct*., **82**, 346-361.

Shen, H. (2008), "Boundary layer theory for the buckling and post-buckling of an anisotropic laminated cylindrical shell, Part II: Prediction under external pressure", *Composite Struct*., **82**, 362-370.

Sridharan, S. and Graves-Smith, T.R. (1981), "Post-buckling analyses with finite strips", *J. Eng. Mech. Div.*, *ASCE*, **107**, 869-887.

Wang, S. and Dawe, D.J. (1999), "Spline FSM post-buckling analysis of shear deformable rectangular laminates", *Thin-walled Struct*., **34**, 163-178.